Table S1. Primers used in this study.

R41A-F	gcgcgagggtgcgcagctacgggaagcggcgg
R41A-R	gcgcaccctcgcgcccacggcggccaccttcaa
R44A-F	gccggagggtggccagctacgggaagcggcgg
R44A-R	ggccaccctccggcccacggcggccaccttcaa
L432W-F	acacaatggacaccatttaatggctatgctggagcaaag
L432W_R	aaatggtgtccattgtgtgattttgcaaaccagaagtcca
I391W_F	aaaaaatggataacttatgacctgattaaatatgatgtggagaaa
I391W_R	gtcataagttatccatttttttctgtaggtagtttactcttcc
I392W_F	aaaaaaatctggacttatgacctgattaaatatgatgtggagaaa
I392W_R	gtcataagtccagatttttttctgtaggtagtttactcttcc
Fatp2b_F	acaggtgctactcttgccttgcggactaaattttcag
Fatp2b-R	caagagtagcacctgtggttccagaagtataaatgtata
EcoRI_Nter_FATP2	ccggaattcatgctttccgccatctacaca
XbaI_Cter_FATP2	ctagtctagacttatcgtcgtcatccttgtaa
V36W-F	aagtgggccgccgtgggccggagggtgcgcagc
V36W-R	cacggcggcccacttcaagaagtagcctatgtcctg
A37W-F	aaggtgtgggccgtgggccggagggtgcgcagc
A37W-R	cacggcccacaccttcaagaagtagcctatgtcctg
V39W-F	aaggtggccgcctggggccggagggtgcgcagc
V39W-R	ccaggcggccaccttcaagaagtagcctatgtcctg
L248W-F	actggctggacttttgtaagcggattgaaggcagatgat
L248W-R	tacaaaagtccagccagttccataccatatgcgctgatg
I391W-I392W-F	aaaaaatggtggacttatgacctgattaaatatgatgtggagaaa
I391W-I392W-R	gtcataagtccaccatttttttctgtaggtagtttactcttcc
L432W-F	acacaatggacaccatttaatggctatgctggagcaaag
L432W-R	aaatggtgtccattgtgtgattttgcaaaccagaagtcca
R42A_F	gcgcgagggtgcgcagctacgggaagcggcgg
R42A_R	gcgcaccctcgcgcccacggcggccaccttcaa
R41A-R42A-R44A_F	gcgcggccgtggccagctacgggaagcggcgg
R41A-R42A-R44A_R	ggccacggccgcgcccacggcggccaccttcaa
K48A_F	ggggcgcggcggccggcgcgcaccatcctgcg
K48A_R	ggccgccgcgccccgtagctgcgcaccctccgg
R49A_F	gggaaggcccggccggcgcgcaccatcctgcg
R49A_R	ggccgggccttcccgtagctgcgcaccctccgg
R50A_F	gggaagcgggcaccggcgcgcaccatcctgcg
R50A_R	ggtgcccgcttcccgtagctgcgcaccctccgg
K48A-R49A-R50A_F	ggggcggccgcaccggcgcgcaccatcctgcg
K48A-R49A-R50A_R	ggtgcggccgccccgtagctgcgcaccctccgg
R41A/R42A/R44A/K48A/R49A/R50A_F	gccagctacggggcggccgcaccggcgcgcaccatcctg
R41A/R42A/R44A/K48A/R49A/R50A_R	cgccccgtagctggccacggccgcgcccacggcggcca

Table S2. Statistics for data collection and refinement

	FATP2 C18-AMP	FATP2 Lipofermata
PDB	28KF	28KR
EMDB	EMD-56574	EMD-56581
Data collection and processing		
Magnification	105,000	105,000
Voltage (kV)	300	300
Electron exposure (e–/Å^2)	42	42
Defocus range (μm)	2.0 - 0.8	2.0 - 0.8
Pixel size (Å)	0.836	0.836
Symmetry imposed	C1	C1
Initial particle images (no.)	12,718,109	13,705,110
Final particle images (no.)	211,297	135,106
Map resolution (Å)	3.68	3.70
FSC threshold	0.143	0.143
Map resolution range (Å)	3.2 - 5.0	3.2 - 5.1
Refinement		
Initial model used (PDB code)	AF2	AF2
Model resolution (Å)	3.78	4.00
FSC threshold	0.50	0.50
Model composition		
Non-hydrogen atoms	10,059	4995
Ligands	42	21
B factors (Å^2)		
Protein	58.77	52.33
Ligand	47.54	36.50
R.m.s. deviations		
Bond lengths (Å)	0.005	0.004
Bond angles (°)	0.604	0.942
Validation		
MolProbity score	1.85	2.23
Clashscore	7.10	11.09
Poor rotamers (%)	0.19	1.70
Ramachandran plot		
Favored (%)	92.75	91.71
Disallowed (%)	0.16	0.16

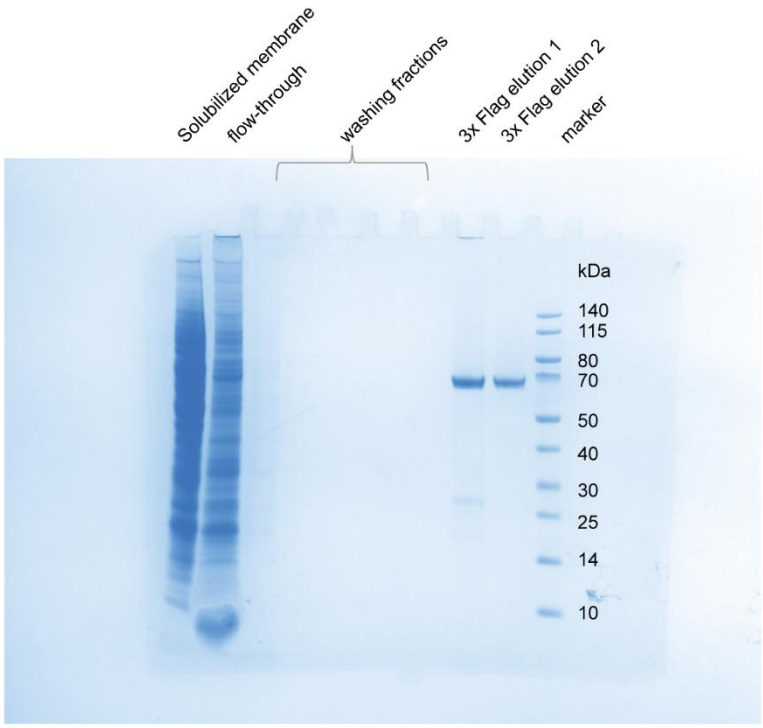

Supplementary Fig. 1. Purification of human FATP2. Uncropped SDS-PAGE of purification for Flag tagged FATP2. PageRuler pre-stained protein ladder shows FATP2 band at 70 kDa on a NuPAGE Bis-Tris mini protein gel (4–12%, 1.0–1.5 mm). Similar results were obtained for all purification performed.

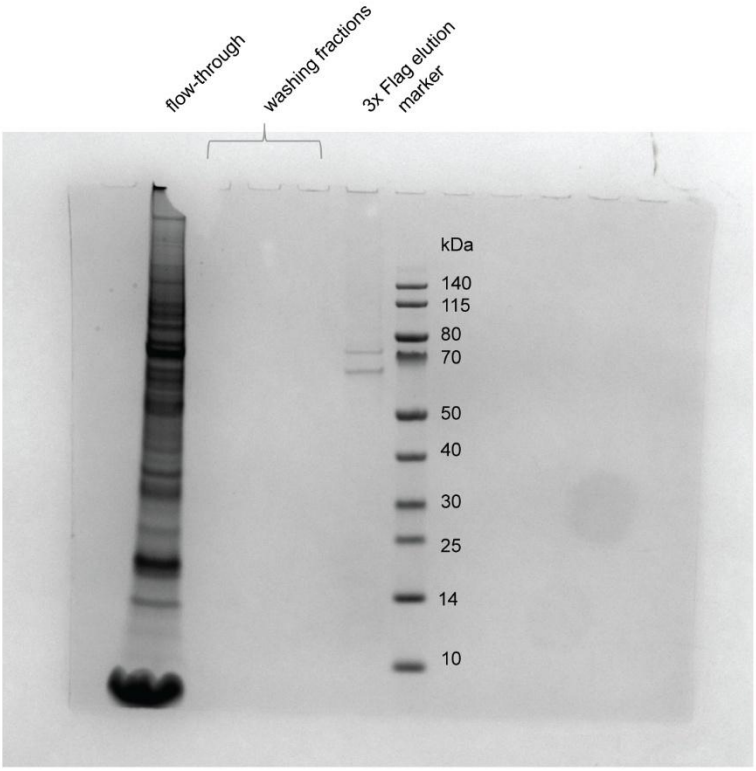

Supplementary Fig. 2. Purification of human FATP2b. Uncropped SDS-PAGE of purification for Flag tagged FATP2b. PageRuler pre-stained protein ladder shows FATP2b band below 70 kDa on a NuPAGE Bis-Tris mini protein gel (4–12%, 1.0–1.5 mm). A band slightly above 70 kDa marker is likely HSP70.

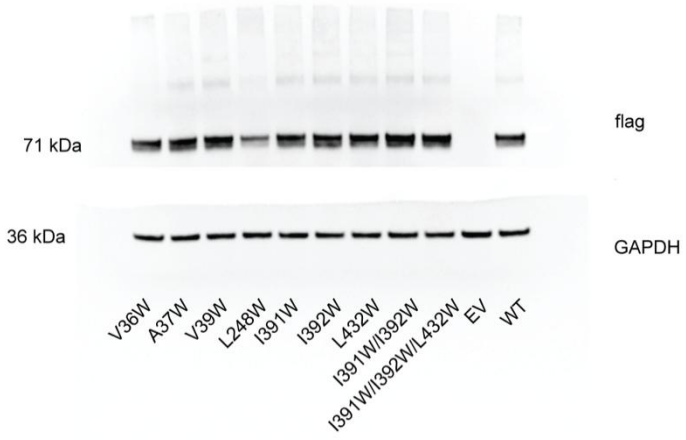

Supplementary Fig. 3. Uncropped western blots of tunnel mutants. After transfer, membranes were cut into half prior to blocking and antibody incubation. The top half was probed with anti-flag antibody and bottom were probed with anti-GAPDH antibody. Experiments were repeated three times (n=3) and quantified using ImageJ.

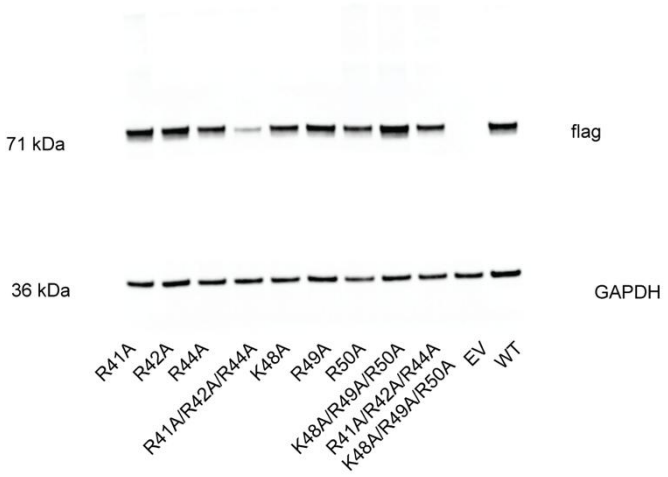

Supplementary Fig. 4. Uncropped western blots of APH mutants. After transfer, membranes were cut into half prior to blocking and antibody incubation. The top half was probed with anti-flag antibody and bottom were probed with anti-GAPDH antibody. Experiments were repeated three times (n=3) and quantified using ImageJ.

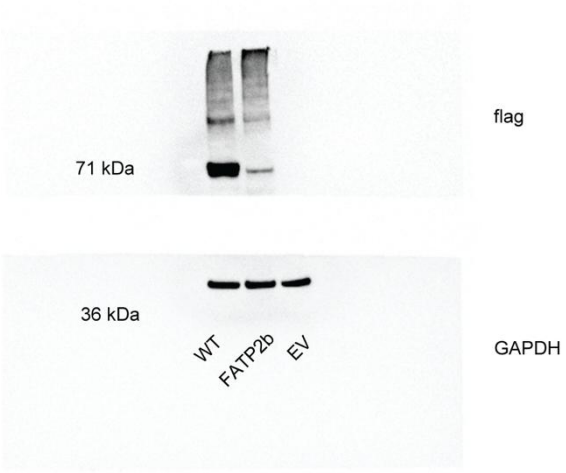

Supplementary Fig. 5. Uncropped western blots of FATP2b. After transfer, membranes were cut into half prior to blocking and antibody incubation. The top half was probed with anti-flag antibody and bottom were probed with anti-GAPDH antibody. Experiments were repeated three times (n=3) and quantified using ImageJ.

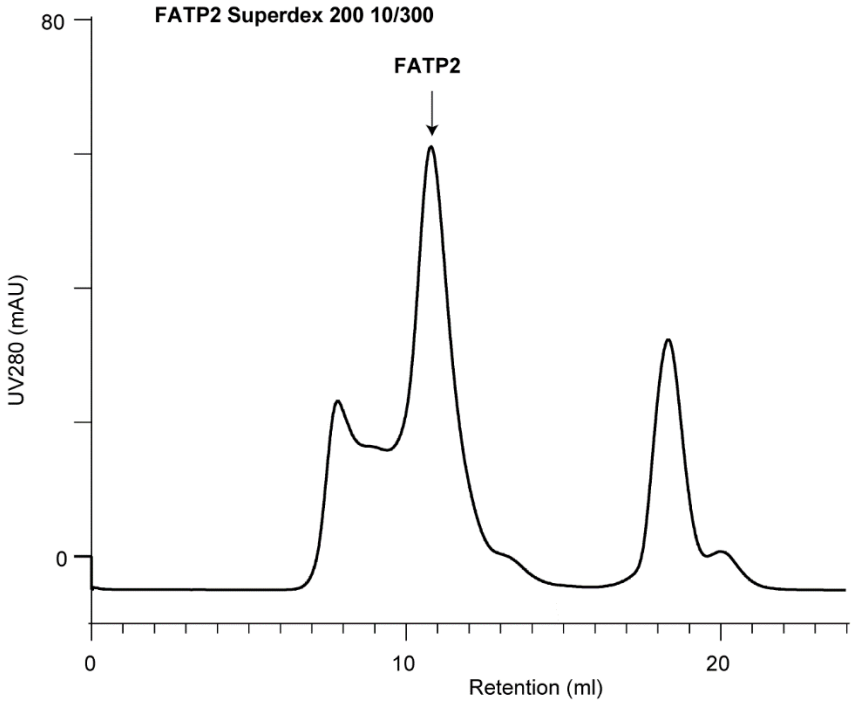

Supplementary Fig. 6 Elution profile of FATP2 on a size exclusion chromatography column (Superdex 200 Increase 10/300) in 25 mM HEPES pH 7.0 buffer containing 150 mM NaCl, 0.02% DDM and 0.002% CHS. FATP2 is eluted at ~11 ml. Similar results were obtained for all purification performed.

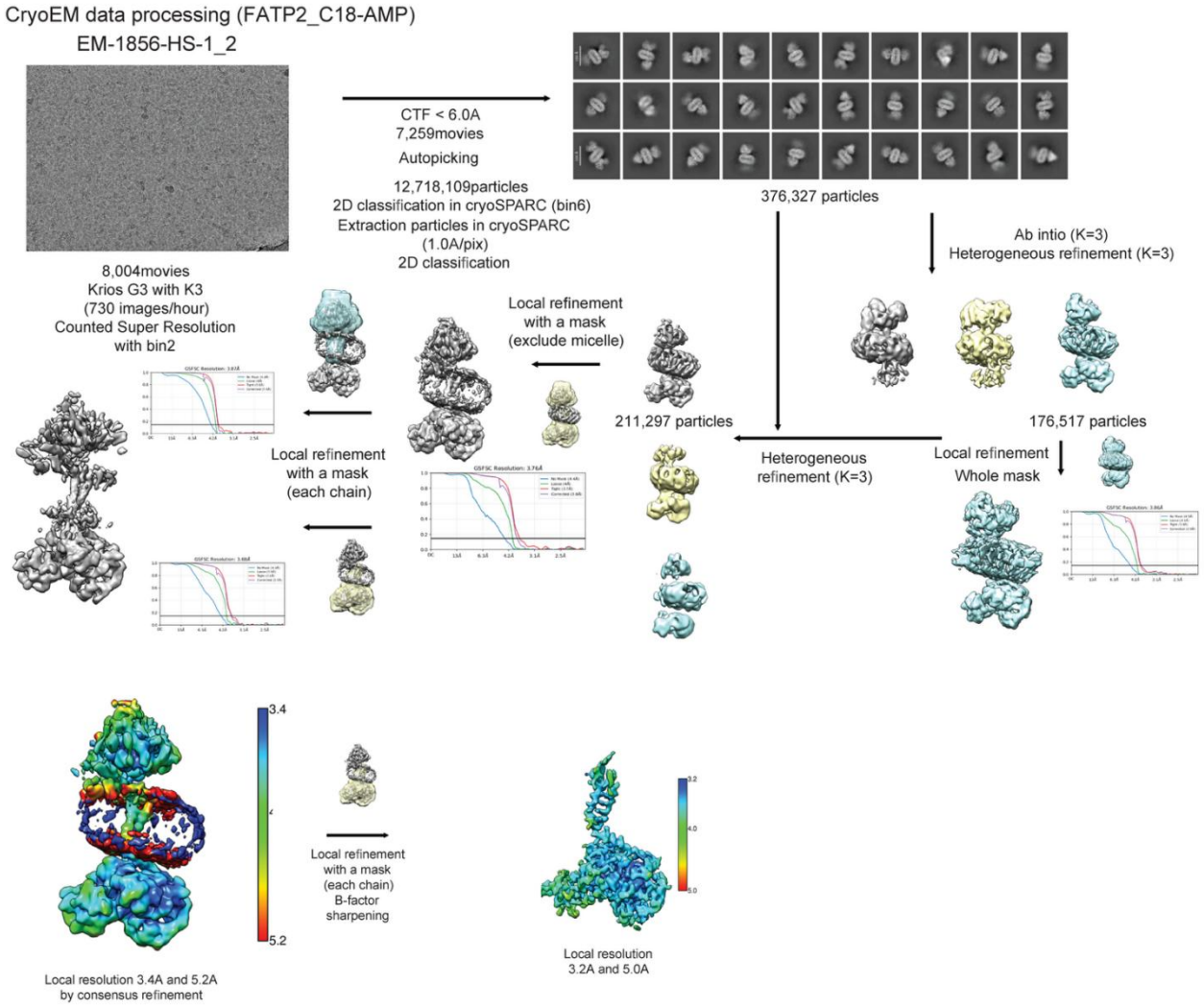

Supplementary Fig. 7. Cryo-EM processing workflow and classification for FATP2 in complex with adenylate intermediate.

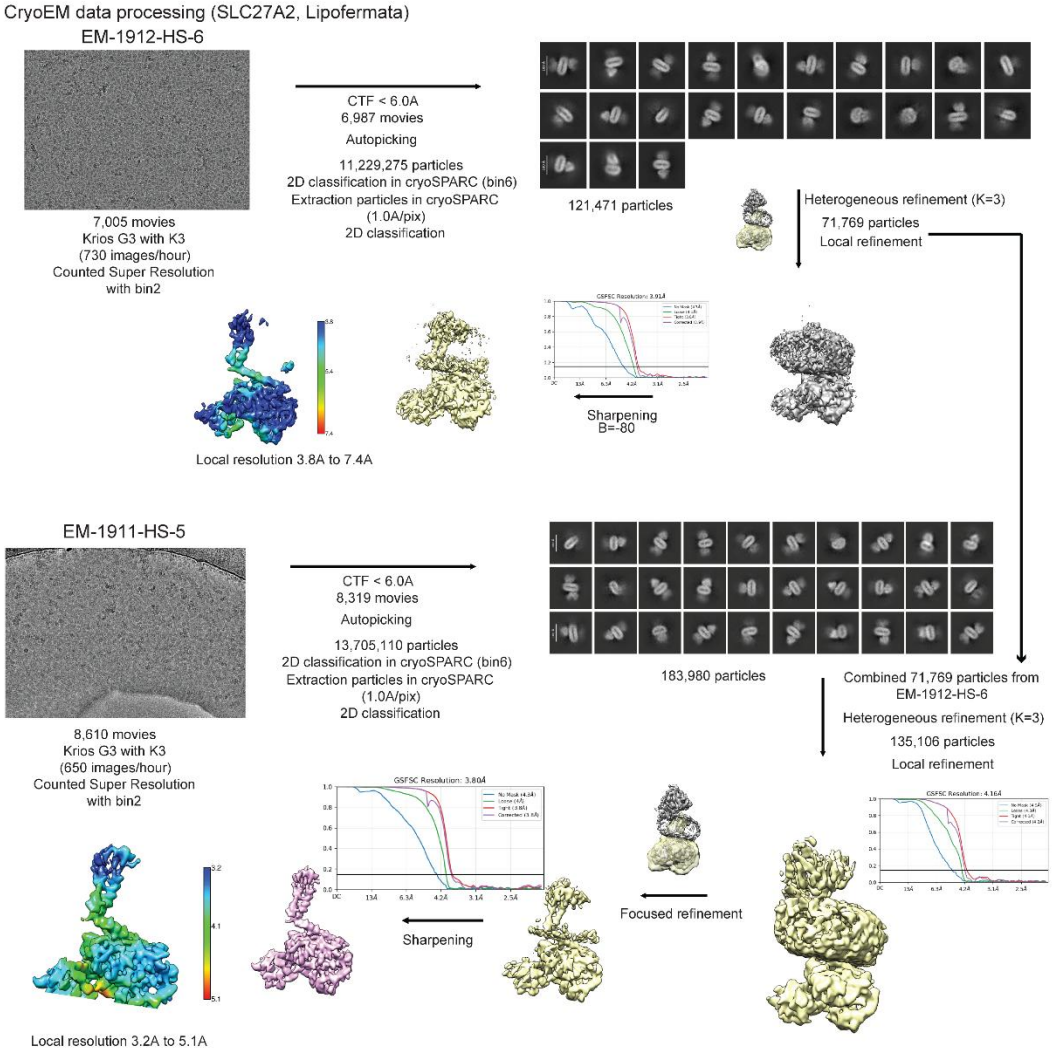

Supplementary Fig. 8. Cryo-EM processing workflow and classification for FATP2 in complex with lipofermata.

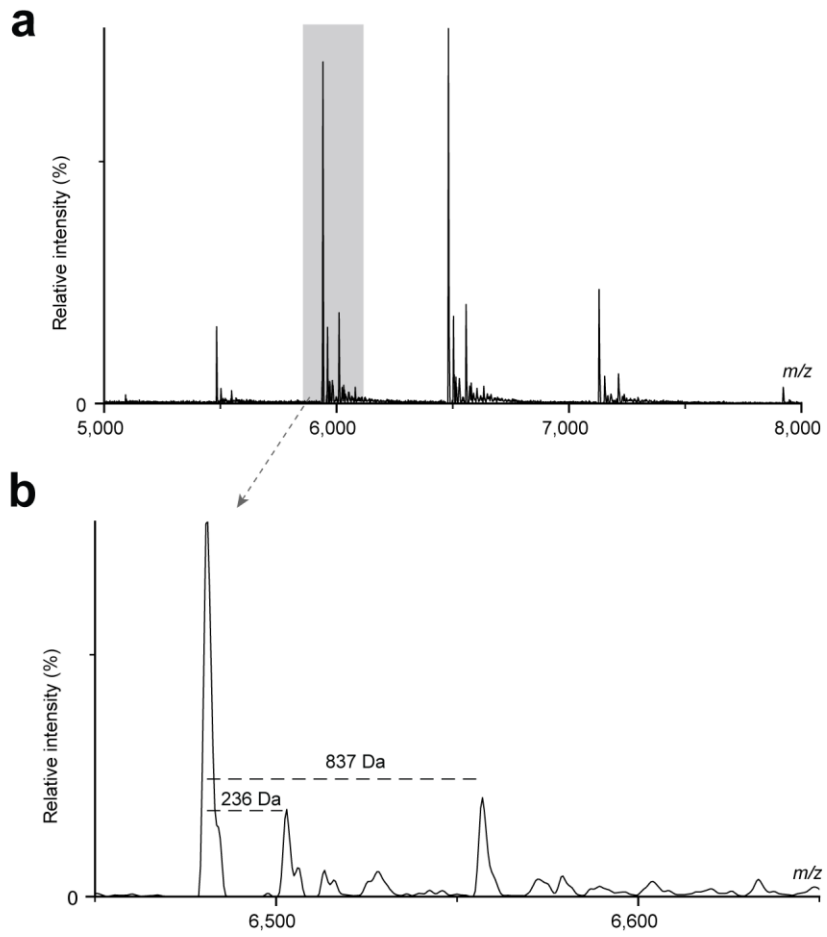

Supplementary Fig. 9. nMS spectrum of FATP2 under negative mode shows mass shift of +236 Da, consistent with palmitoylation. a. nMS spectrum of FATP2 within m/z range of 5,000-6,000. **b**. Focused view of FATP2 at the 18^- charge state.

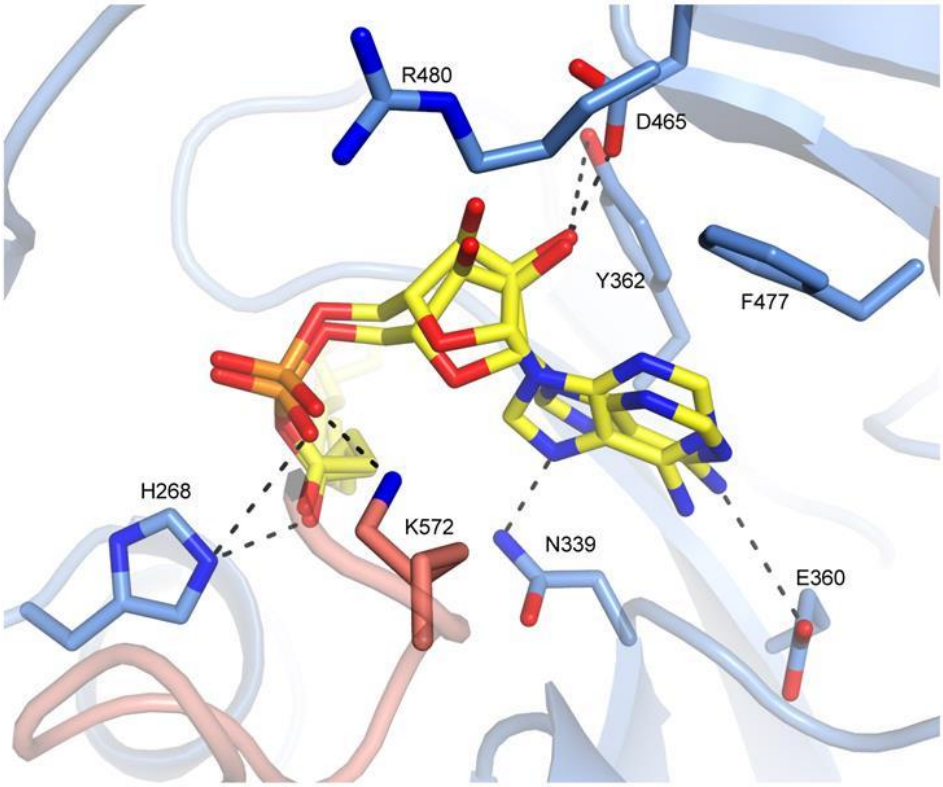

Supplementary Fig. 10. Binding site for AMP moiety in the adenylate intermediate complex structure. Cartoon is shown in blue for central domain and salmon for C-terminal domain. Dash line denotes hydrogen bonds.

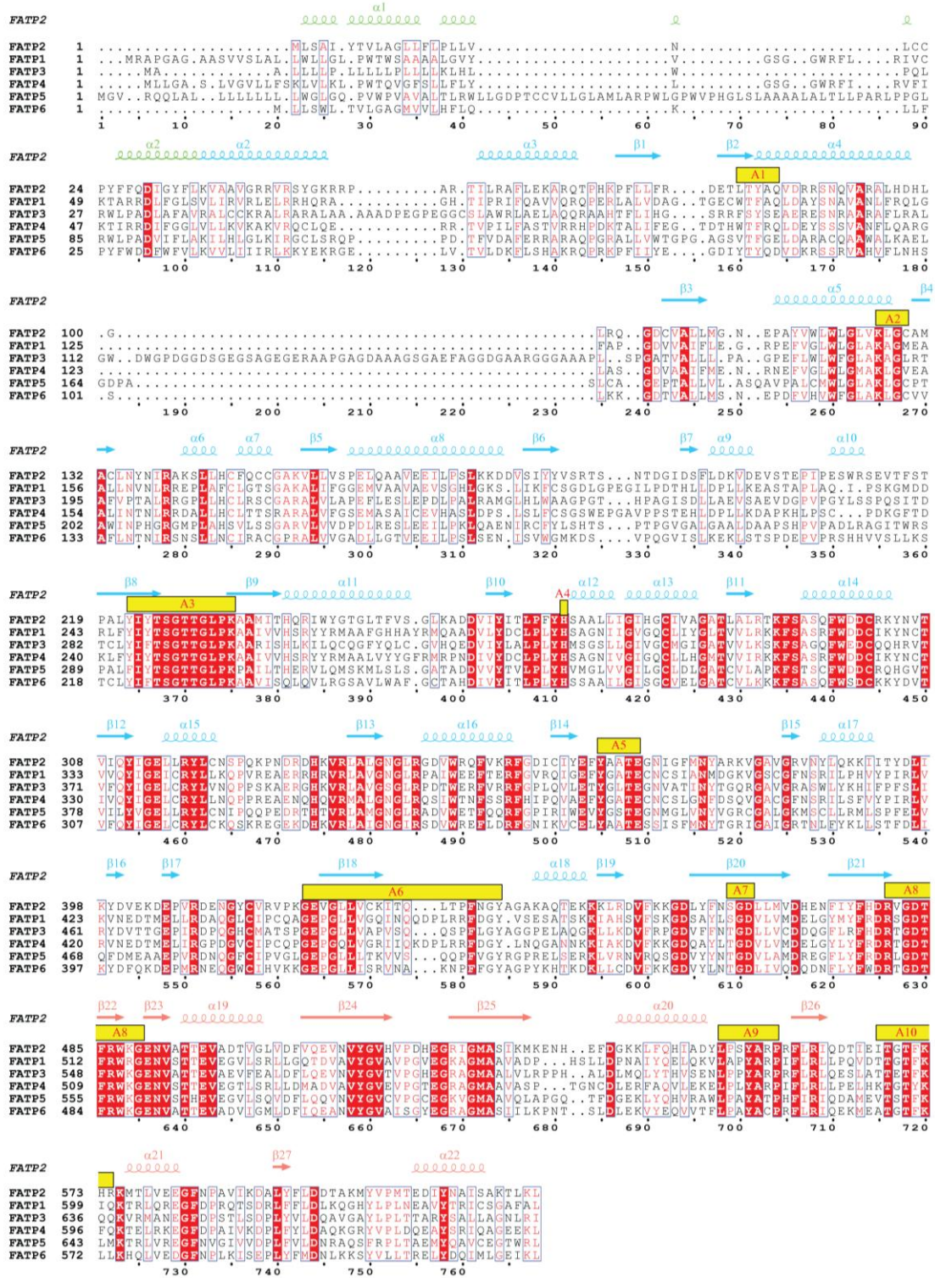

Supplementary Fig. 11. Secondary structure assignment of FATP2 with anchoring helix (green), central domain (blue), and C-terminal domain (red). Alignment was prepared in MUSTUNG[1] and rendered with ESPript 3.0[2] with secondary structure of FATP2 depicted above the sequence alignment with the following colouring rule: red box with white character, strict identity; red character, similarity; blue frame, similarity across groups. Motifs conserved among ANL family enzymes are highlighted in yellow squares.

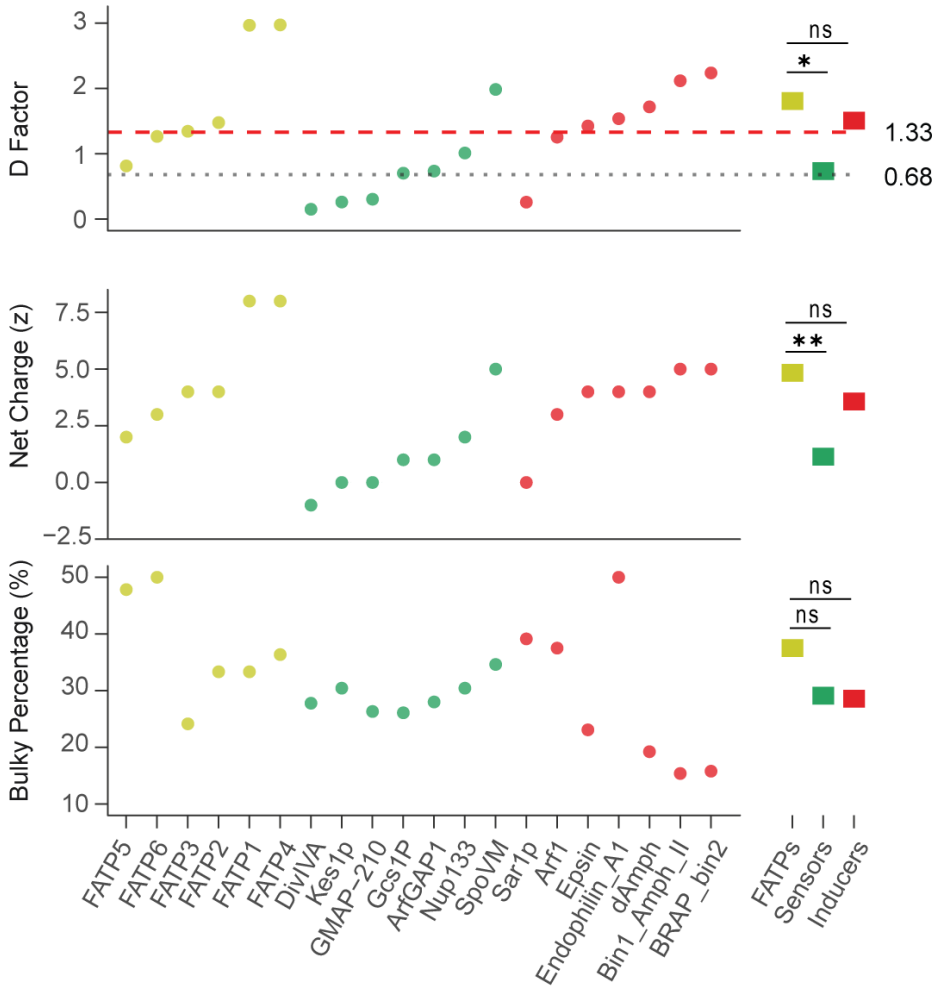

Supplementary Fig. 12. Analysis of amphipathic helices from FATPs, ALPS sensors, and curvature inducers. The scatter plot shows D-factor, net charge and overall density of bulky residues.

1 Konagurthu, A. S., Whisstock, J. C., Stuckey, P. J. & Lesk, A. M. MUSTANG: a multiple structural alignment algorithm. *Proteins* **64**, 559-574 (2006). https://doi.org:10.1002/prot.20921

2 Robert, X. & Gouet, P. Deciphering key features in protein structures with the new ENDscript server. *Nucleic Acids Res* **42**, W320-324 (2014). https://doi.org:10.1093/nar/gku316